Journal of Applied Polymer Science

Effect of Reinforcement of Sustainable β-$CaSiO_3$ Nanoparticles in Bio-Based Epoxy Resin System

Boniface J. Tiimob, Vijaya K. Rangari, Shaik Jeelani
Department of Materials Science and Engineering, Tuskegee University, Tuskegee, Alabama 36088
Correspondence to: V. K. Rangari (E-mail: rangariv@mytu.tuskegee.edu)

ABSTRACT: The β-$CaSiO_3$ nanoparticles (NPs) were prepared using calcium carbonate from egg shells and silica as precursors. These NPs were incorporated (1–4 wt %) into bio-based epoxy resin to fabricate nanocomposites. Thermal and mechanical tests were carried out on these composites. The results of dynamic mechanical analysis showed significant improvement in the storage modulus of 1 and 2 wt % composites. The thermomechanical analysis data revealed ~19 and 20% of reduction in coefficient of thermal expansion for 1 wt % of $CaSiO_3$ before and after glass transition as compared to the neat epoxy system. Thermogravimetric analysis results also showed delayed thermal degradation of the composites by significant amounts (17–35°C) for 5% of decomposition, a proportional increase in residues corresponding to the loading concentrations. The flexure tests showed significant improvements in strength (17–36%), modulus (5–33%), and toughness for 1–4 wt % of reinforcement of β-$CaSiO_3$ NPs. Theoretical calculations of the reinforcement effect on the flexure modulus of the composites agree well with the experimental values. The scanning electron micrograph of the fractured surfaces revealed better interfacial interactions in the composites and enhancements in crack path deflections over the neat specimen. © 2014 Wiley Periodicals, Inc. J. Appl. Polym. Sci. **2014**, *131*, 40867.

KEYWORDS: biocomposite; biodegradable; biomaterials; biopolymers & renewable polymers; nanocomposite

Received 2 February 2014; accepted 9 April 2014
DOI: 10.1002/app.40867

INTRODUCTION

The evolution of composite technology in recent times has led to the development of functional hybrid materials with properties falling in between those of the inferior and superior parent materials. These composite materials are indispensable in the aerospace industry, marine, armor, automobile, railways, civil engineering structures, sport goods, and many others.[1] Polymers are poor in stiffness and strength by nature. To enhance these properties for advanced applications, particulate fillers, such as micron or nano-SiO_2, glass, Al_2O_3, Mg $(OH)_2$, and $CaCO_3$ particles, carbon nanotubes, and layered silicates, are often added to polymer composites.[1] These composites combine the advantages of their different constituent phases, size-dependent, and surface properties to improve the deficient properties of polymers.[2] It has been reported that phased matrix based on polymers and montmorillonite (MMT) exhibits unexpected properties such as reduced gas permeability, improved solvent resistance, enhanced mechanical-, and flame-retardant properties.[1,3] Similar investigations also showed that epoxy resins modified with inorganic particles such as carbon, TiO_2, SiO_2, Al_2O_3, and clay demonstrated improved performances.[3,4] In composites, the size of particles and the interfacial adhesion immensely influence the mechanical properties of the matrix. Good dispersion of inorganic fillers in a polymer matrix and their affinity to organic phases significantly determine the overall improvement in performance.[5] The use of nanosized materials in high-performance polymers for property modification has shown considerable promise. Different from micron-sized fillers which are consumed in quantities of more than 30 wt % to effect significant improvement, considerable improvement can be achieved with <10 wt % of exfoliated nanosized fillers.[1]

Reports emphasize that calcium silicate is one of the most versatile, functional filler with unique properties which can enhance the performance of plastics, paints and coatings, construction, friction and ceramic materials, as well as in metallurgical applications.[6,7] Though ceramic materials possess high compressive strength, $CaSiO_3$ ceramics which are used in these applications are unfortunately very brittle and poor in tensile and torsional properties.[8] Owing to the challenging as well as the advantageous properties of bioceramics and polymers, a good approach is to combine these materials to obtain hybrids with intermediate properties. The use of β-$CaSiO_3$ as filler in polymers showed promise in improving mechanical properties, mostly in thermoplastic but similar application in thermosetting polymers is very limited, probably due to economic constraints on production in the sol–gel and rock mining processes. This

can be resolved by resorting to cheap sources like the egg shell for the production of β-$CaSiO_3$ NPs in a more sustainable way for filler applications. Hence, we derived β-$CaSiO_3$ NPs (<50 nm) from egg shells and silica through ball milling and sonochemical method and incorporated specific quantities into thermosetting polymer to alter its microstructure for enhanced thermal and mechanical properties for advanced applications. The polymer used in this study is a bio-based epoxy, Super sap® 100/1000. Super sap® 100/1000 was chosen because it contains 37% of biorenewable materials as coproducts from wood pulp and biofuel production, unlike conventional epoxies which are primarily made from petrochemicals.[9] This helps in advancing our goal of developing environmentally sustainable materials from biowaste. The natural components in this resin exhibit excellent elongation and very good adhesive properties. The ability to fast cure at room temperature and low content of sensitizing ingredients improve user's safety. These make it more advantageous over conventional epoxy systems. Also, the relative medium viscosity and great adhesion to most substrates make it an excellent resin for composites. The biorenewable content suggests the use of green chemistry which eliminates or reduces adverse environmental impacts. The material safety data sheet[10] indicates that it can potentially reduce carbon monoxide and greenhouse gas emissions by a minimum of 50%. This earned it the United States Department of Agriculture (USDA) BioPreferred℠ Product classification using ASTM D6866.[11] The choice of this resin supports global efforts on conducting environmentally benign research on alternative functional materials to satisfy societal needs. Attempts to produce bio-based materials using natural fibers and bio-based resins have been made, but such environmentally friendly composites suffer from several limitations such as low mechanical properties due to low strength in reinforcement, and inadequate interfacial bond strength.[12] NPs have shown significant potential as reinforcement in many polymer materials and can be used in the bio-based formulations for potential property enhancements. Hence, improvement in mechanical properties can be explored with the bio-sourced β-$CaSiO_3$ NP which is one of the most suitable fillers because of its low absorption to moisture as opposed to the challenge in high moisture absorption by most natural reinforcement and the bio-based epoxies.[13]

MATERIALS AND METHODS

Synthesis and Characterization of $CaSiO_3$ Nanofiller

The β-$CaSiO_3$ was synthesized from egg shell and amorphous SiO_2 by ball milling about 10 g of 1 : 1 ratio ($CaCO_3$: SiO_2) for 100 min in an 8000D mixer-mill. The ball milling was carried out in two separate canisters which contained ~5 g each of the precursors and eight pieces of 6-mm diameter steel balls. About 6 g of the mixture was then sintered to 1000°C at a rate of 10°C/min and allowed to stay for 3 h and then cooled at the same rate to room temperature in a vacuum tube furnace (GLS-1300X). The solid product (~3.5 g) was then crushed in a ceramic mortar and ball milled again for 10 h using liquid polypropylene glycol as the medium. It was then washed four times with absolute ethanol and centrifuged at 12,000 rpm for 10 min in Beckman Coulter (ALLEGRA-64R). This was then dispersed by mixing with absolute ethanol to a volume of 50 mL and sonicating with Sonics vibra cell ultrasound (WCX 750) at an amplitude of 50%, at 25°C for 3 h, then centrifuged at 12,000 rpm in Beckman Coulter (ALLEGRA-64R) and vacuum dried for 24 h.

X-ray diffraction (XRD) analysis of $CaSiO_3$ was carried out to confirm its crystal structure using D-max 2100 X-ray diffractometer. This test was carried out at 40 KV and 30 mA, 5°C/min sampling rate, sampling width of 0.020 and 3 to 80, 2θ°.

Transmission electron microscopy (TEM) was carried using a Joel 2010 microscope. The sample was prepared by dispersing 1 mg powder sample in 5 mL of absolute ethanol for 10 min in an ultrasonic bath and placing a drop of the colloidal solution of the specimen on a copper grid and used for analysis.

Fabrication of Super Sap® 100/1000 epoxy/β-$CaSiO_3$ Nanocomposites

In this study, β-$CaSiO_3$ NPs were used to reinforce a bio-based epoxy resin developed by Entropy Resin (San Antonio, CA, USA) to evaluate the effect of the NPs on their thermal and mechanical properties on the composites. The Super Sap® 100/1000 system is composed of Super Sap® 100 epoxy, a modified, liquid epoxy resin, with Super Sap®1000 hardener. Different from conventional epoxy systems that are composed mainly of petroleum-based materials, Super Sap® formulations contain biorenewable materials sourced as coproducts or from waste streams of industrial processes, such as wood pulp and biofuel production. Study specimens were prepared by mixing a ratio of 2 : 1 of Parts A and B for each batch of specimen. Approximately, 100 g of Part A was measured into a plastic beaker, the required weight percent of NPs (1, 2, 3, and 4) was added and magnetically stirred at 1200 rpm for 8 h to achieve uniform mixing. The mixture was then transferred into a 300-mL sample holder and 48 g of Part B was added, mixed, and defoamed for 3 min each at 1200 and 1000 rpm, respectively, in a Thinky mixer (Model ARE-250). This was then poured into standard silicone rubber molds for flexure (13 mm (w) × 89 mm (l) × 5 mm (t)) and dynamic mechanical analysis (DMA) (15 mm (w) × 60 mm (l) × 5 mm (t)) specimen and left to cure at a controlled room temperature of 25°C for 24 h and postcured at 48.8°C for 2 h in an Isotem oven 200 series (Model 230F). They were then allowed to cool to 25°C for 3 h. These were cut and sand to the standard dimensions for thermomechanical analysis (TMA), DMA, thermogravimetric analysis (TGA), and flexure tests.

Thermal Characterization of the Nanocomposites

Dynamic Mechanical Analysis. DMA instruments allow the application of a dynamic force in addition to the static force of TMA on to a specimen. In the DMA, the phase lag between an applied dynamic force and the response yields a complex modulus, which can be mathematically separated into storage or in-phase elastic response E' and loss or out-of-phase viscous response E''.[10] All DMA samples were cut to approximately 60 × 12 × 3.5 mm, according to ASTM Standards (D4065-06).[14] These dimensions were obtained by rotor sanding under constant flow of water to avoid the damage of the specimen surface by the sandpaper. DMA was done using TA Q 800 equipment purge with N_2 gas at a flow rate of 50 mL/min and a frequency of 1 Hz in a three-point bending mode. The average sample dimensions

(thickness and width) were entered and analyzed by ramping at a rate of 5°C/min to 150°C. TA universal software was used to analyze the results for storage modulus.

Thermomechanical Analysis. TMA is a technique for determining dimensional changes in materials. It is very accurate in the measurement of expansion and contraction of materials such as nanocomposites.[15] In a TMA experiment, a probe is lowered onto the surface of a sample and the movement of the probe is measured as the sample gets heated. With a load applied to the probe, a combination of modulus change and expansion of the sample are observed. Depending on the probe to sample contact area and the load applied, the glass transition (T_g) can be detected by either an upward (expansion) or a downward (penetration) movement of the probe. With large contact areas and low forces, expansion is primarily observed, whereas for small contact areas and high forces penetration is primarily observed. Coefficient of thermal expansion (CTE) is determined by the ratio of change in dimension per unit dimension and change in temperature, and this is designated as $(\Delta l/L)/\Delta T$ where Δl is the change in length, L is the original length, and ΔT is the change in temperature.[16] The effect on dimension changes due to the incorporation of $CaSiO_3$ NPs in the epoxy matrix was evaluated using TA Q 400 equipment in the expansion mode. Each of the three specimens was cut to about 10 × 10 × 5 mm and analyzed under inert N_2 gas atmosphere at a flow rate of 50 mL/min and ramped at 5°C/min to 150°C with a constant probe force of 0.2 N. CTE [α] was determined at specific ranges before (30–70°C) and after (110–140°C) the T_g regions by using the slope of the line of best fit method in the TA universal software.

Thermogravimetric Analysis. TGA was performed to evaluate the effects of $CaSiO_3$ NPs on the thermal stability of the composite. This was done by using TA Q500 equipment. A specimen weight of approximately 12 mg each was used in the test. The tests were run in a N_2 gas atmosphere at a flow rate of 60 mL/min, ramped at 10°C/min up to 600°C. The data were retrieved and analyzed using TA universal software.

Flexure Test

Flexure testing is an important characterization process for many materials because it provides relevant information on the material's response under real application. Especially for composite materials which are often used in aerospace, automotive, and other structural applications; it is critical to understand how much flex the material can tolerate and still maintain its strength. The flexure test involved specimen with the span-to-thickness ratio, l/d, chosen to produce flexure failure. The specimen dimensions were 89 mm × 12.7 mm × 3.7 mm. This gave the recommended span-to-thickness ratio of 16, and a span length of 60 mm. ASTM D790-10,[17] standard test method B, was followed to execute the test as the polymer system has high toughness and undergoes large deflections during testing. In this test, the specimen is deflected until tensile or compressive rupture occurs, or the maximum specimen strain is reached. Data from six specimens of each nanocomposite were averaged and used for the analysis. The thickness, length, and width of each sample were measured using a digital caliper. The thickness of the middle portion of each specimen was used in the test, whereas the width was

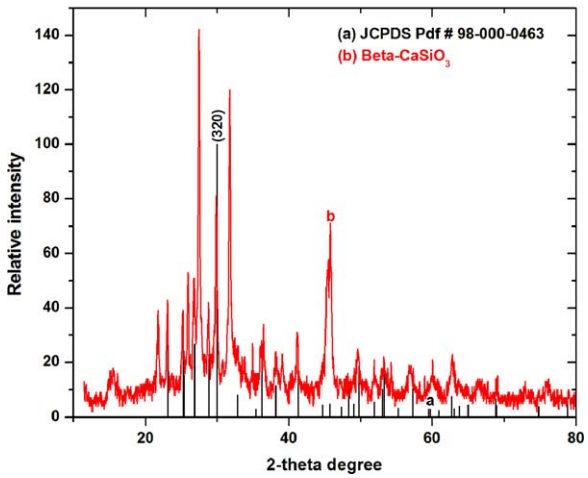

Figure 1. XRD pattern of (a) $CaSiO_3$ standard and (b) synthesized $CaSiO_3$ NPs.[Color figure can be viewed in the online issue, which is available at wileyonlinelibrary.com.]

an average measurement along the length of each specimen. The strain rate for this test was 0.10 mm/mm/min as specified by ASTM D790-10 method B.[17] The crosshead motion rate of 1.6 mm/min was used based on the specimen thickness and span length. Based on the results of the three-point bending test, load versus deflection (stress vs. strain) curves can give all the important information needed to determine the flexure strength and modulus as well as other mechanical properties as desired. The flexure strength as determined by the equipment makes use of the equation: $S = 3Pl/2bd^2$ where P is maximum failure load, l is support span, b is width of specimen, and d is thickness, whereas the flexural modulus is computed using $E = l^3m/4bd^3$ where m is slope of the tangent to the initial straight-line portion of the load deflection curve. This test was done using Zwick/Roell Z2.5 material testing system with 2.5 kN of load cell. The distance between separations of the two supports (span length) was set to 60 mm on the support scale, based on the l/d ratio of the specimen. Test parameters were entered according to ASTM Standard D790-10.[17] The crosshead speed of 1.6 mm/min and strain rate of 0.10 mm/mm/min were used in the analysis.

Scanning electron microscopy (SEM) microstructure analysis of the fractured surface dispersion, fracture mode, nature of surface, as well as microstructures of the neat and nanocomposites was characterized using SEM JEOL JSM-5800 operated at 10 KV. The fractured samples were cut and held with carbon tape on a 4-in wide sample holder of the SEM. This was then sputter coated with gold–palladium for 5 min in Hummer 6.2 sputtering system purged with N_2 gas and operated at 20 mT, 5 V, and 15 mA.

RESULTS AND DISCUSSION

XRD and TEM Characterization of the Synthesized $CaSiO_3$ NPs

The XRD pattern of the final product is shown in Figure 1(b). This reveals prominent peak intensities at Bragg's angles, $2\theta^\circ$ = 23.2, 25.3, 26.8, 28.9, 30.0, 32.9, 35.4, 36.2, 38.2, 39.1, 41.3, 44.7, 45.7,47.3, 48.3, 49.1, 49.7, 51.9, 53.1, 53.3, 55.2, 57.3, 59.5, 62.7, 65.0, 68.9, 74.8, and 78.8. These angles correspond, respectively, to the crystal planes (400), (002), (20-2), (202),

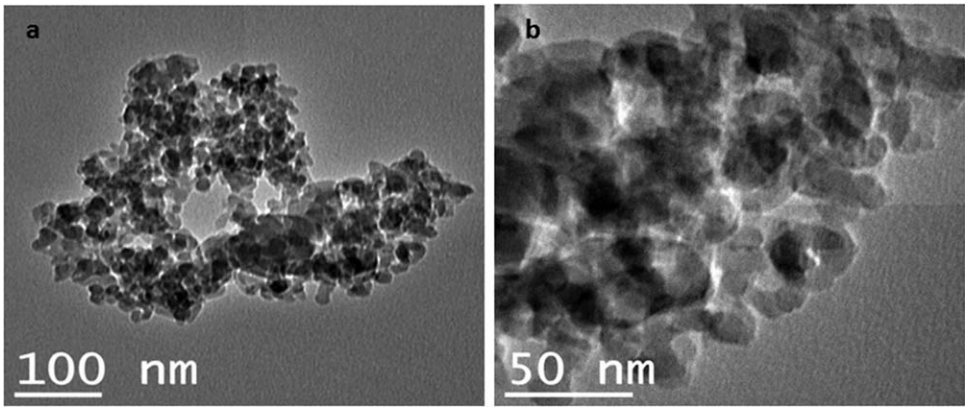

Figure 2. Transmission electron micrograph of the synthesized $CaSiO_3$ NPs. (a) Low magnification and (b) high magnification.

(320), (40-2), (42-1), (122), (520), (20-3), (521), (52-2), (603), (800), (720), (72-1), (040), (004), (52-3), (72-2), (341), (722), (32-4), (324), (24-3), (10, 0,2), (044), and (92-4) of standard β-$CaSiO_3$ phase in an ascending order of the diffraction angles. It matches very well with the Joint-Committee-on-Powder-Diffraction-Spectra (JCPDS) Pdf file #98-000-0463 [Figure 1(a)] as well as the literature findings on $CaSiO_3$, especially the position of the parent (signature) peak at (320) crystal plane.[18–20] The TEM micrographs in Figure 2(a,b) show the $CaSiO_3$ NPs with sizes of <50 nm. This confirms that polycrystalline $CaSiO_3$ NPs as revealed by the XRD were obtained in the process.

Thermal and Mechanical Properties of the Nanocomposites

Thermogravimetric Analysis. The effect of $CaSiO_3$ NPs on the thermal stability of the composite was evaluated using TGA. The onset of decomposition, first (minor) and second (major) decomposition temperatures, temperatures at 5 and 50% weight loss, and residues were determined. These results are summarized in Table I. As shown in Figure 3(a), the polymer has two different maximum transitions. This suggests double degradations of two components with different thermal stabilities. The first (minor) decomposition is a component of 37% of biorenewable content, whereas the major degradation (second) is due to the degradation of the more stable components.

The thermogram shown in Figure 3(a) is the full thermal profile of $CaSiO_3$-filled nanocomposite from which portions with major changes have been plotted separately to show magnified views of these changes. These portions clearly show the trends in thermal decomposition. The addition of $CaSiO_3$ NPs revealed improvement ranging from 1 to 3°C in onset temperature and significant delays of about 17–35°C on 5% of decomposition temperature [Figure 3(b)]. Another enhancement of about 3–6°C was realized at 50% of weight loss and it is shown in Figure 3(c). Zhou et al.[1] found a 6°C increase in decomposition temperature of 1–4 wt % carbon/clay/epoxy nanocomposites compared to the neat carbon/epoxy. This suggests that the 17–35°C improvement, we found, is very significant compared to their findings though different silicates were used in both cases. The residue at 550°C also showed an increasing trend from the lowest load to the highest which is shown in Figure 3(a). The improvement in the onset, 5 and 50% of degradation, as shown in the shift of the curves to the higher temperatures in their respective region on the percentage weight loss curves in Figure 3(b,c) can be associated with the high thermal stability of $CaSiO_3$ which is capable of shielding heat energy from rapid transfer to the polymer molecules not in direct contact with the particles.

The TGA of polypropylene–clay composite showed that degradation took place at a higher temperature in the presence of clay.[21] This was associated with a diffusion effect, which impedes the emission of the gaseous degradation products, resulting in an increase in the thermal stability of the material. It was further elaborated that the clay enhanced thermal stability by acting as a mass transport barrier to the volatile product

Table I. Effect of $CaSiO_3$ on the Thermal Stability of Super Sap® 100/1000 Epoxy System

Specimen	Onset of major decomposition	Decomposition temperature (°C)		Maximum decomposition temperature (°C)		Residue at 550°C %
		At 5 wt %	At 50 wt %	First	Second	
Neat	327.54 ± 2.11	186.20 ± 5.80	375.80 ± 0.85	201.75 ± 0.63	371.27 ± 1.36	3.73 ± 0.47
E + 1% $CaSiO_3$	328.04 ± 2.58	217.15 ± 3.61	379.95 ± 1.05	208.88 ± 2.94	370.04 ± 0.22	5.33 ± 0.12
E + 2% $CaSiO_3$	330.42 ± 0.78	216.15 ± 10.54	378.30 ± 0.85	200.81 ± 1.05	369.43 ± 0.42	5.71 ± 0.19
E + 3% $CaSiO_3$	328.91 ± 0.62	203.20 ± 0.57	379.75 ± 0.32	190.93 ± 2.43	368.95 ± 1.03	6.71 ± 0.03
E + 4%$CaSiO_3$	330.05 ± 0.88	221.00 ± 1.84	381.21 ± 0.41	200.29 ± 2.28	371.48 ± 0.54	9.28 ± 0.78

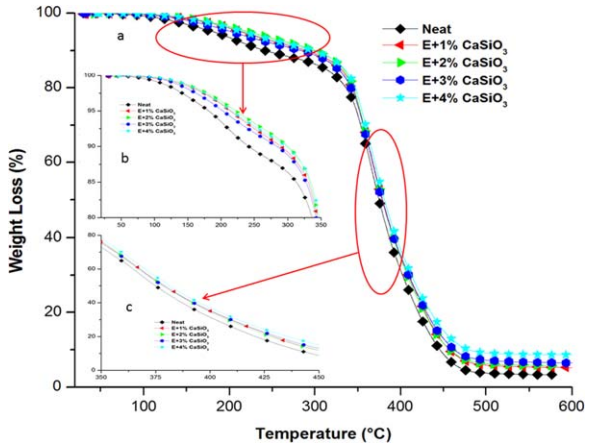

Figure 3. TGA thermographs showing the effect of $CaSiO_3$ NPs on the thermal stability of Super Sap® 100/1000 epoxy system. [Color figure can be viewed in the online issue, which is available at wileyonlinelibrary.com.]

generated during decomposition, as a result of a decrease in permeability.[21] This suggests that the nanostructure is critical to the improvement of thermal stability of nanocomposite materials and our results on different nanosilicate support this finding. Also, Liang et al.[22] found that MMT possessed high thermal stability and its layer structure advantageously exhibited great barrier which hindered the evaporation of the small molecules generated during the thermal decomposition and slowed the decomposition of the photosensitive polyamide matrix.[22] This further suggests that with good dispersion of $CaSiO_3$, similar property enhancement is achievable though $CaSiO_3$ is not layered like MMT to influence the properties isotropically. The residue measured at 550°C showed an increasing trend as the NP amount increased. This shows that the decomposition is reduced at the increase of the NPs from one level to another. Hence, fire retardancy of the composite is enhanced by the presence of the NPs. Also, the remnants of the matrix (char) contributes to the amount of residue. As the onset, 5 and 50% decomposition, temperatures showed improvements, the char yields owing to the delayed degradation of the matrix was higher in the composites in a proportional manner compared to that of the neat system.

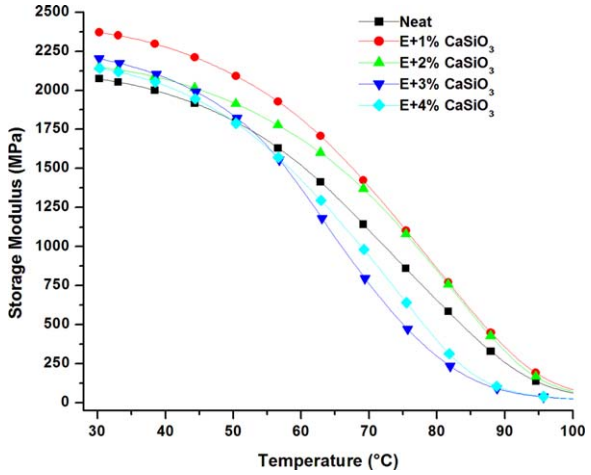

Figure 4. Storage moduli of Super Sap® 100/1000 epoxy system infused with $CaSiO_3$ NPs. [Color figure can be viewed in the online issue, which is available at wileyonlinelibrary.com.]

The formation of char at the initial stage is a key reason for the improvement of the decomposition temperatures and the residue. Char formation has been sited to be responsible for the impermeability of volatile-degraded components that have the potential to accelerate combustion.[21,23]

Dynamic Mechanical Analysis. Storage modulus, the ability of a material to store mechanical energy when subjected to variations in temperature, was measured for the neat epoxy system and the nanocomposites. This was used to evaluate the effect of the NPs on the damping properties of the polymer. The results of this test shown in Figure 4 reveals that the addition of $CaSiO_3$ NPs led to enhancements in the storage moduli of the nanocomposites over that of the neat epoxy system from room temperature to 50°C. The maximum improvement in this property was observed in 1 wt % loaded specimen (296.76 ± 55.58 MPa). However, further increment in $CaSiO_3$ loads (2–4 wt %) showed a decreasing trend from that of 1 wt %. After 50°C, the storage moduli for 3 and 4 wt % of loaded specimen fell below that of the neat as shown in Figure 4. This indicates brittleness in the specimen and the inability to elastically store energy above this temperature. The probability of an increase in the number of agglomerates as the concentration of particles increases becomes higher with NPs. This is one reason why the storage modulus decreased in such a trend. The earlier reports of the DMA on nanocomposites with MMT revealed significant improvements in the storage moduli of polymers, such as PVDF, PP, and PMMA.[24–26] Zhou et al.[1] also found a phenomenal increase in the storage modulus in 1–4 wt % carbon/clay/epoxy nanocomposites compared to the neat carbon/epoxy. Our findings support theirs' in the case of 1–2 wt % of loading, but also show that higher loads (3–4 wt %) can compromise the damping properties of the matrix.

Improvement in the storage modulus has been attributed to enhancements in the rigidity of polymer molecules which restricts their movement with increase in temperature, good dispersion of nanofillers into the structure of polymers, and the strength of the interface affinity between the matrix and the fillers.[27,28]

Thermomechanical Analysis. In determining the effect of $CaSiO_3$ NPs on the dimensional change in Super Sap® 100/1000 epoxy system, the CTE in specimens at each load category was determined using an expansion mode in the temperature ranges between 30–70 and 110–140°C before and after the T_g region, respectively. The results of these analyses are shown in Figure 5 (dimension change) and Figure 6 (bar plots of CTEs).

The incorporation of $CaSiO_3$ NPs improved the dimensional stability of the epoxy resin by a minimum of 10% (2 wt % loading) and a maximum of 19% (1 wt % loading) compared to that of the neat system before the T_g region as shown in Figure 6. The addition of 3–4 wt % of $CaSiO_3$ showed ~17% of reduction in CTE which is a significant improvement. Though

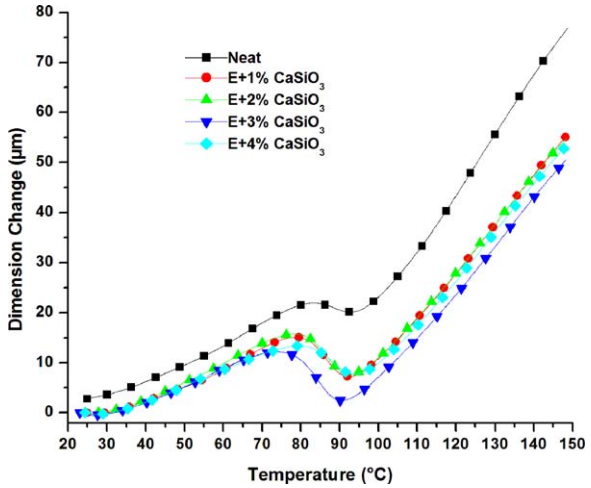

Figure 5. Dimension changes of Super Sap® 100/1000 epoxy composite. [Color figure can be viewed in the online issue, which is available at wileyonlinelibrary.com.]

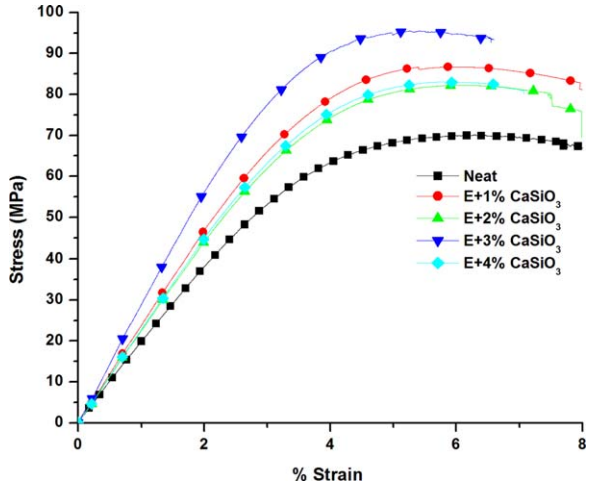

Figure 7. Flexure behavior of $CaSiO_3$–Super Sap® 100/1000 epoxy composite. [Color figure can be viewed in the online issue, which is available at wileyonlinelibrary.com.]

the other specimens showed reductions in CTE, it is desirable to obtain optimum improvements with a small quantity of a nanomaterial. Hence, the CTE reduction by about 19% at 1% of loading of $CaSiO_3$ is good because higher concentration can greatly compromise the strength and toughness of the matrix. The CTE determined after the T_g region compares well with those obtained before, though the percentage changes which ranged from 12 to 20% were slightly higher than those determined before the T_g for the various respective specimens. The CTEs of conventional epoxy filled with 50 wt % of seven different inorganic compounds and cured with two different hardeners showed reduction ranging from 6.98 to 37.98% in CTEs.[29] This suggests that our finding is significant, with just 1–4 wt % of $CaSiO_3$ giving maximum improvements of 19 and 20% before and after T_g, respectively.

In Figure 5, the results of the nanocomposite show straight-line regions with slopes lower than that of the neat system. This indicates increased dimensional stability. Past reports have shown that inorganic reinforcing fillers are stiffer than the matrix and highly resistant to deformation, and hence their inclusion causes an overall reduction in the matrix strain; especially, in the area near the particle as a result of the particle to matrix interface while increasing the dimensional stability.[30] In support of this, the CTEs of composites based on matrices such as polyamide-6, polypropylene, and polyamides[15,22,31,32] have been found to be lower than those of their respective neat polymers, especially with the incorporation of small amount of organically modified montmorillonite.[33,34] Reports also show that the trend in the amount of CTE reduction depends on the particle rigidity, on the dispersion of the clay platelets in the matrix, and also on an efficient stress transfer to clay layers. It is believed that the retardation of chain segmental movement through incorporation of organically modified clays also leads to decrease in the CTE.[34]

Flexure Test

The flexural strength and modulus of $CaSiO_3$–Super Sap® 100/1000 epoxy composites were evaluated using the three-point bending test. The results are shown in the stress–strain plots of Figure 7, and the derived mechanical properties are shown in Figure 8. This shows an improvement in flexure strength, elastic

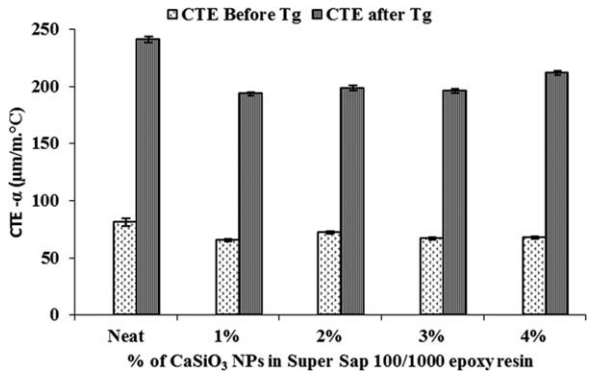

Figure 6. The mean and standard deviation values of CTE of Super Sap® 100/1000 composite.

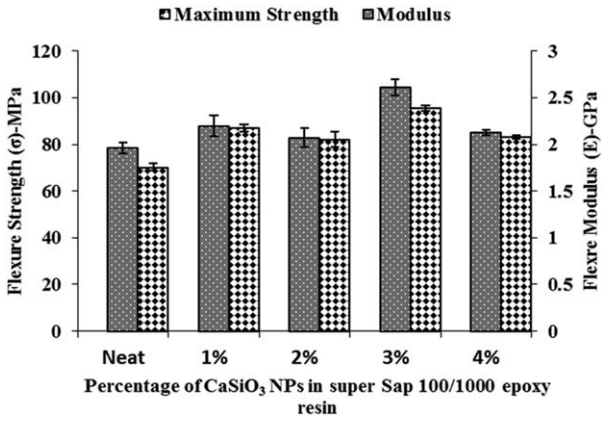

Figure 8. The mean and standard deviation values of flexure strength and modulus of $CaSiO_3$–Super Sap® 100/1000 epoxy composites.

modulus, and toughness of the $CaSiO_3$–bio-based epoxy nanocomposites compared to the neat epoxy system.

As shown in Figure 8, the percent improvements in flexure strength ranges from 17.12 to 36.22% owing to 1–4 wt % of loading of $CaSiO_3$ NPs into the matrix. This is promising in the sense that the maximum strength of the neat epoxy system as reported by the manufacturer is 77 MPa but our findings revealed a maximum strength of about 70.21 MPa. An improvement ranging from 5.22 to 18.64 MPa still exists if these results are compared to the manufacturer's reported maximum strength of 77 MPa though our comparison is made with a maximum strength of 70.21 MPa. The inability to reproduce the manufacturer's data is due to the differences in skill levels, equipment used, changes in environmental conditions under which specimen were prepared, and tested among others.

Similarly, the trend in the improvement of flexure modulus matches those in flexure strength with respect to the specific loading. The improvement in modulus is much in 3 wt % loading of $CaSiO_3$, followed by 1, 4, and 2 wt % loads, respectively (Figure 8). This shows that 3 wt % loading of $CaSiO_3$ NPs gave the best improvement in strength and modulus among the specimens. One striking property which informed the choice of the Super Sap® 100/1000 epoxy system is its exceptional toughness over other epoxy systems. This is because our reinforcement material is a bioceramic and very brittle in nature, and since the matrix has good toughness, the improvement of other properties of the composite could be explored without much compromise in the material's toughness. The stress–strain curve in Figure 6 clearly shows that flexure strength, modulus, and toughness have been considerably improved with the addition of $CaSiO_3$ NPs. Even at a test speed of 16 mm/min, there is no sign of failure up to 6% of strain. Though the failure occurred in the samples with 3 and 4% loadings of $CaSiO_3$, this happened after 6% of strain, and suggests that the composite retains its improved toughness even beyond the acceptable maximum strain of 5% emphasized in ASTM Standard.[17] Hence, the adverse effect of the brittle ceramic particles may not be felt during the application of the composite unlike other conventional systems that become very brittle and susceptible to failure. Improvement in strength and modulus suggests that favorable interactions may have been established between the NPs and the polymer matrix such that more energy or load is required to cause the failure of composite material than it is required to cause similar effects in the neat specimen. Zhou et al.[1] found about 13.5% of improvement in flexural strength of 1–4 wt % of carbon/clay/epoxy nanocomposites.

Reports have shown that improvement in strength depend on the ease in stress transfer between the reinforcement materials and the matrix.[35] Applied stress is effectively transferred between particles and matrix in instances where good adhesions exist and lead to enhancement in the strength.[35] Major contrasts of reduction in strength occur when the interaction is very poor or the particle sizes are large.[36]

It has also been demonstrated that polycaprolactone composite films containing 5 wt % of $CaSiO_3$ and Na_2CaSiO_4 submicron particles (250 nm) showed improved nanotopography, increased compressive stiffness, and elastic modulus under quasi-static compression load.[7] Again, an investigation on both unmodified and surface-modified β-$CaSiO_3$ particles with dodecyl alcohol dispersed in poly(DL-lactic acid) (PDLLA) matrix improved the tensile strength of the composite over the neat PDLLA.[8] On the other hand, Zhang and Chang[37] found that electrospun composite with modified β-$CaSiO_3$ nanowires and unmodified β-$CaSiO_3$ showed that the unmodified β-$CaSiO_3$ in poly(butylene succinate) matrix decreased the tensile strength in a trend proportional to increased β-$CaSiO_3$ content. However, the tensile stresses of composite due to modified β-$CaSiO_3$ revealed an increase of about 40% compared to those containing unmodified β-$CaSiO_3$.[37] This suggests that the differences in matrix affect their affinity to the particles and will either require surface modifications or not. Furthermore, the evaluation of diisocyanate-modified bioglass NPs (diameter, ~40 nm) in poly(L-lactide) (PLLA) revealed improvement in the tensile strength (56.7–69.2 MPa as a result of the addition of 4 wt %), tensile modulus, and impact energy of the composites due to increased phase compatibility. Also, they found that the structure of a fractured surface of this composite was surface grafted with well-dispersed bioactive glass in the PLLA matrix.[38] Another investigation on a scaffold with varying wollastonite content revealed that strength significantly increased by the addition of 50% of sintered wollastonite phase.[39] Also, β-$CaSiO_3$ has outstanding filler properties such as binding properties, strength, modulus, and low CTE. It is thermally insulating, incombustible, and less moisture absorbing.[40]

One issue with thermosetting resins is their extreme brittleness but it has been found that inorganic particles have good toughening mechanisms that help subdue this brittleness in composites.[2] Though improvement in toughness is insignificant compared to that of rubber inclusions, improvement in modulus and hardness has been enormous.[2] The extent of enhancement in mechanical properties of composites resulting from the addition of fillers depends on the particle size, particle–matrix interface adhesion, and how good the particles are dispersed in the matrix. Reports emphasize that smaller $CaCO_3$ particles lead to increase in strength of filled polypropylene and high-fracture toughness in high-density polyethylene composites.[41] This supports our finding with $CaSiO_3$ which has a similar structure to $CaCO_3$. Perhaps, because C and Si belong to the same periodic group and demonstrate similar reactivity.

The effect of the nanofiller in the composite was determined theoretically and compared with the experimental results. These calculations were carried out using the Halpin–Tsai rules of mixture, eqs. (1) and (2).[42–44]

$$\frac{1}{E}=\frac{\varnothing_f}{E_f}+\frac{1-\varnothing_f}{E_m} \quad \text{(for lower bound)} \tag{1}$$

$$E=\varnothing_f E_f+E_m(1-\varnothing_f) \quad \text{(for upper bound)} \tag{2}$$

where E = modulus of composite, $\varnothing_f$ = $CaSiO_3$ (filler) volume fractions, E_f = $CaSiO_3$ (filler) modulus, and E_m = modulus of matrix (epoxy).

Filler effect ($CaSiO_3$ NPs) on the modulus of the bio-based epoxy matrix is compared to the calculated moduli based on

Table II. Theoretical and Experimental Effect of $CaSiO_3$ on the Super Sap® 100/1000 epoxy

Specimen	Filler volume fraction ($\varnothing_f$)	*E*—calculated (lower limit)	*E*—calculated (upper limit)	*E*—experimental (flexure)
E + 1% $CaSiO_3$	0.004	1.97	2.30	2.20 ± 0.11
E + 2% $CaSiO_3$	0.008	1.98	2.60	2.07 ± 0.10
E + 3% $CaSiO_3$	0.012	1.98	2.96	2.61 ± 0.09
E + 4% $CaSiO_3$	0.016	1.99	3.30	2.13 ± 0.03

the theoretical modules of rules of mixtures by Halpin–Tsai (Table II). The theoretical moduli, *E*, of the composites were calculated using $CaSiO_3$ modulus (E_f = 85.2 MPa) from literature[45] and the $CaSiO_3$ volume fractions ($\varnothing_f$) and modulus of matrix (E_m) used in our experiment. The lower limits of the theoretical values were obtained using Haplin–Tai's eq. (1), whereas the upper limits were evaluated using eq. (2). The experimental moduli are those obtained from flexure analysis of the composites. The experimental results agree well with those from the theoretically moduled equations. It is evident that the experimental flexure moduli fall within the lower and upper limits of the calculated theoretical values. The differences between the theoretical values and the experimental values because theoretical modules assume ideal conditions of uniform shape, constant dimensions, unidirectional, good bonding, uniform modulus, and dispersion of the filler. However, the reality

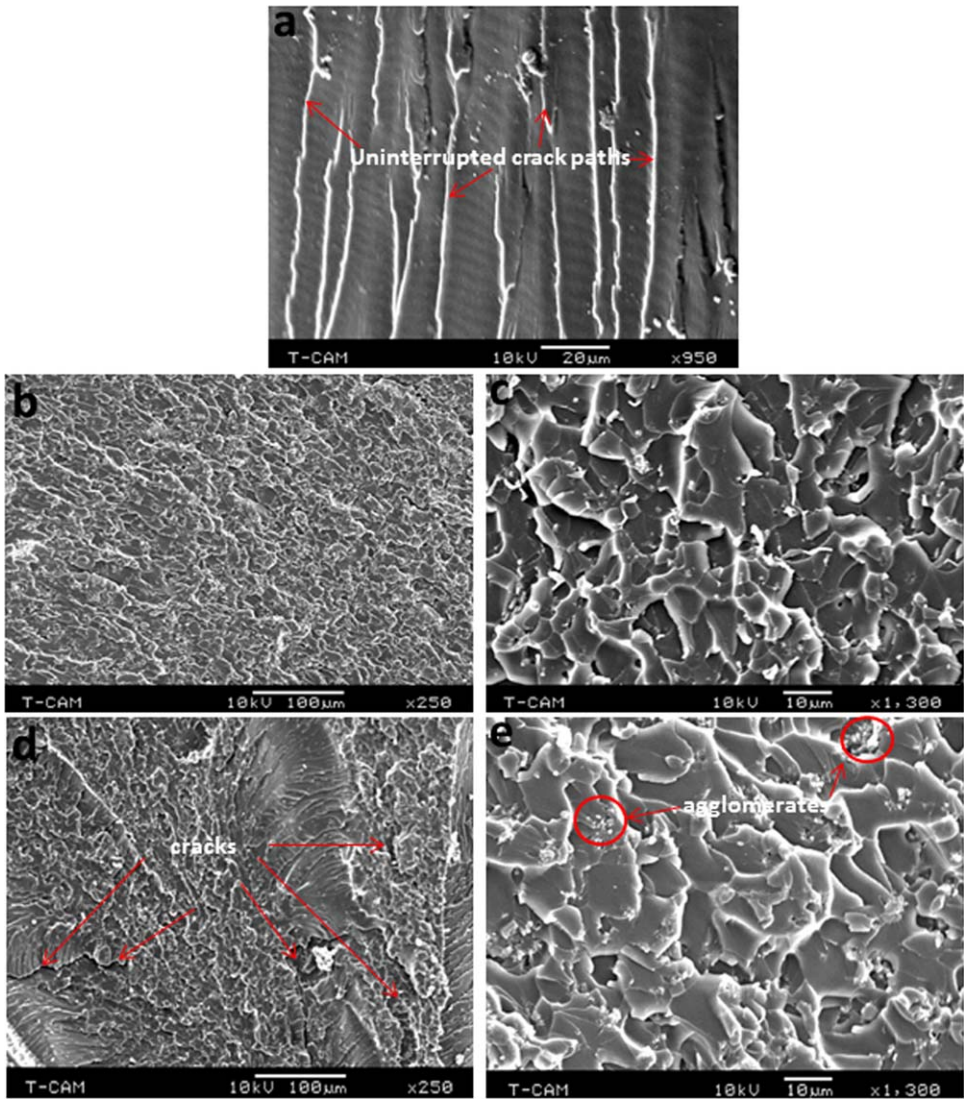

Figure 9. SEM micrograph showing the microstructure of the fractured surface (a) neat, (b,c) 3 wt % $CaSiO_3$ NPs, and (d,e) 4 wt % of $CaSiO_3$ NPs. [Color figure can be viewed in the online issue, which is available at wileyonlinelibrary.com.]

in experiments is quite different and complex; fillers can be nonuniform in shape, length, and thickness, misaligned, agglomerated, and weakly bonded, and can change in morphology among others.[44]

SEM Analysis of Fractured Surfaces of the Nanocomposites

The fractured surfaces were probed through a scanning electron microscope. The micrographs in Figure 9 show the fractured surface of the neat sample and those of the nanocomposites with two different filler concentrations after the flexure test.

The fracture surface of the neat specimen does show smooth vertical paths owing to the cracks which propagated across the thickness direction as evident in the micrographs shown in Figure 9(a). The pallets seen at isolated portions in this micrograph are pieces of the polymer which cracked partially, but still loosely bound to the fractured surface. The nature of this fractured surface suggests a brittle failure mode because the crack propagation is uninterrupted. The failed surfaces of the nanocomposites show rough ridge patterns and river markings on the fracture surface as shown in Figure 9(b,c). The roughness of the fracture surface is an indication of crack path deflection and ductile nature of the cracks. The fractured surface microstructure reveals cracks and particles spread on the entire surface. It is clear that the mode of crack propagation is very different from that of the neat specimen. The rough ridge patterns and river markings, suggesting that the cracks propagated around these shapes to delay failure during the flexure test. This is the reason for the improved toughness over the neat system. The surfaces also show areas with microvoids, agglomerates, and cracks in the composite. These are evident in the micrographs for the 4 wt % loaded composite [Figure 9(d,e)] and explains the reason why its mechanical properties fell below that of 3 wt % loaded. Agglomerate and voids serve as stress concentration points in materials. It has been found that voids drastically reduce the strength and modulus as well as causing premature failure, whereas agglomerates reduce strength, toughness, and strain to failure.[34] This revelation suggests that the mechanical properties were compromised to some extent in the composite. Hence, the reported improvements could have been more if voids and agglomerates were eliminated to a large extent.

CONCLUSIONS

The results of XRD and TEM confirmed that nanoscale $CaSiO_3$ was obtained from the waste egg shells and amorphous silica precursors. DMA showed better storage moduli with the incorporation of lower concentrations compared to higher loads of $CaSiO_3$. This means that higher loads made the composite very rigid and brittle, limiting the polymer molecules from flexing. Significant improvement in the dimension stability by the addition of 1 wt % of $CaSiO_3$ also suggests that $CaSiO_3$ can be used as filler, especially in space structure where dimensional stability is a major issue. Also, the evaluation of the thermal profiles of the composites showed that the $CaSiO_3$ NPs can improve the thermal decomposition temperatures of epoxy systems significantly as well as amounts of residue. Flexure strength and modulus revealed significant improvements owing to the incorporation of $CaSiO_3$ NPs. Also, toughness improved considerably below 8% of strain, but the strain to failure was reduced in the composites. This result suggests that the bio-sourced $CaSiO_3$ is good reinforcing filler and can be used to enhance the mechanical properties of materials engineered for both biomedical and structural engineering applications. The SEM micrographs of fractured surfaces for the composites revealed microstructures that are similar in surface roughness and topology, but the nature of these surfaces suggests that $CaSiO_3$ strongly interacted with the matrix. The fracture surface of the neat epoxy system exhibited uninterrupted crack propagation (undeflected crack path), resulting from the brittle failure. In contrast, fractured surface of nanocomposites showed an improved toughness characterized by crack path deflection, rough, and ridge patterns with river marking lines. They revealed that the cracks were interrupted and deflected on the entire cross-section. Hence, the improvement in toughness of the composite was due to the action of phase-separated inorganic fillers as crack-arresting points. The revelations of voids and agglomerates suggest that our reported moduli and strengths are not the optimum attainable improvements and could be further improved. Putting together the various improvements, the justified conclusion is that bio-sourced $CaSiO_3$ NPs are good at enhancing the thermal and mechanical properties of polymers intended for advanced applications. A comparison of the flexure moduli of the composite with those calculated from theoretical equations to examine the filler effects showed good agreement. They should be relied on as an alternative to the unsustainable rock-mined and sol–gel-derived $CaSiO_3$ fillers.

ACKNOWLEDGMENTS

The financial support of the NSF-CREST#1137681, NSF-RISE#1137682 Alabama EPSCoR #1158862, and The Alabama Commission on Higher Education is gratefully acknowledged. The authors are also grateful to American Dehydrated Foods, Atlanta, GA, USA, for providing the egg shells.

REFERENCES

1. Zhou, Y.; Pervin, F.; Rangari, K. V. *J. Mater. Process. Technol.* **2007**, *191*, 347.
2. Fu, Y. S.; Feng, Q. X.; Lauke, B.; Mai W. Y. *Compos. B Eng.* **2008**, *39*, 933.
3. Goertzen, K. W.; Kessler, R. M. *Compos. B Eng.* **2007**, *38*, 1.
4. Lam, K. C.; Lau, T. K. *Compos. Struct.* **2006**, *75*, 553.
5. Sui, G.; Jana, S.; Salehi-khojin, A.; Neema, S.; Zhong, W. H.; Chen, H.; Huo, Q. *Macromol. Mater. Eng.* **2007**, *292*, 467.
6. Beheri, H. H.; Mohamed R. K.; El-Bassyouni, T. G. *Mater. Design.* **2013**, *44*, 461.
7. Tamjid, E.; Bagheri, R.; Vossoughi, M.; Simchi, A. *Mater. Sci. Eng. C* **2011**, *31*, 1526.
8. Zhang, M.; Ye, L.; Gao, Y.; Lv, X.; Chang, J. *Compos. Sci. Technol.* **2009**, *69*, 2547.
9. Entropy Super Sap-100/1000, available from: http://www.entropyresins.com/sites/default/files/SuperSap-100_1000_TDS.pdf (accessed August 20, 2013).

10. Bilyeu, B.; Brostow, W.; Menard, K. P. *J. Mater. Ed.* **2000**, *22*, 107.
11. Annual Book of ASTM Standards, D6866-11. Standard Test Methods for Determining the Biobased Content of Solid, Liquid, and Gaseous Samples Using Radiocarbon Analysis; ASTM International: West Conshohocken, PA, **2011**.
12. Masoodi, R.; El-Hajjar, R. F.; Pillai, K. M.; Sabo, R. *Mater. Design.* **2012**, *36*, 570.
13. Wang, S.; Masoodi, R.; Brady, J.; George, R. B. *J. Renew. Mater.* **2013**, *4*, 279.
14. Annual Book of ASTM Standards, D4065-06. Standard Practice for Plastics: Dynamic Mechanical Properties: Determination and Report of Procedures; ASTM International, **2006**.
15. Krump, H.; Luyt, A. S.; Hudec, I. *Mater. Lett.* **2006**, *60*, 2877.
16. Wang, M.; Liao, Y.; Chen, D. *Polym. Test.* **2013**, *32*, 75.
17. Annual Book of ASTM Standards, D790-10. Standard Test Method for Flexure Properties of Unreinforced and Reinforced Plastics and Electrical Insulating Materials; ASTM International, **2010**.
18. Singh, S. P.; Karmakar, B. *New J. Glass Ceram.* **2011**, *1*, 49.
19. Tsunematsu, S.; Inoue, K.; Kimura, K.; Yamada, H. *Cement Concrete Res.* **2004**, *34*, 717.
20. Xu, S.; Lin, K.; Wang, Z.; Chang, J.; Wang, L.; Lu, J.; Ning, C. *Biomaterials* **2008**, *29*, 2588.
21. Saito, F.; Mi, G.; Hanada, M. *Solid State Ionics* **2007**, *101–103*, 37.
22. Liang, Z. M.; Yin, J.; Wu, J. H.; Qiu, Z. X.; He, F. F. *Eur. Polym. J.* **2004**, *40*, 307.
23. Huang, Y.; Hana, S.; Panga, X.; Dinga, Q., Yan, Y. *Appl. Surf. Sci.* **2013**, *271*, 299.
24. Priya, L.; Jog, J. P. *J. Polym. Sci. Part B: Polym. Phys.* **2003**, *41*, 31.
25. Lei, S. G.; Hoa, S. V.; Ton-That, M. T. *Compos. Sci. Technol.* **2006**, *66*, 1274.
26. Meneghetti, P.; Qutubuddin, S. *Thermochim. Acta* **2006**, *442*, 74.
27. Liu, X.; Wu, Q.; Berglund, L. A.; Lindberg, H.; Fan, J.; Qi, Z. *J. Appl. Polym. Sci.* **2003**, *88*, 953.
28. Lionetto, F.; Maffezzoli, A. *Appl. Rheol.* **2009**, *19*, 23423:1.
29. Glavchev, I.; Petrova, Kr.; Ivanova, M. *Polym. Test.* **2002**, *21*, 177.
30. Ashton, C. H.; Caulfield, F. D.; Chouzouri, G.; Clemons, M. C.; Davidson, T.; Dey, K. S.; Duca, J.; Flaris, V.; Goyal, A.; Iqbal, Z.; Kamena, K.; Mack, H.; Mascia, L.; Monte, J. S.; Patel, H. S.; Rothon, N. R.; Todd, B. T.; Weissenbach, K.; Xanthos, M. Functional Fillers for Plastics, Part I; Wiley-VCH Verlag GmbH & Co. KGaA: Weinheim, **2005**; p 1.
31. Yoon, P. J.; Fornes, T. D.; Paul, D. R. *Polymer* **2002**, *43*, 6727.
32. Shen, L.; Lin, Y.; Du, Q.; Zhnog, W. *Compos. Sci. Technol.* **2006**, *66*, 2242.
33. Corcione, E. C.; Frigione, M. *Materials* **2012**, *5*, 2960.
34. Asif, A.; Rao, V. L.; Saseendran, V.; Ninan, K. N. *Polym. Eng. Sci.* **2009**, *49*, 756.
35. Reynaud, E.; Jouen, T.; Gauthier, C.; Vigier, G.; Varlet, J. *Polymer* **2001**, *42*, 8759.
36. Tjong, S. C.; Xu, S. A. *J. Appl. Polym. Sci.* **2001**, *81*, 3231.
37. Zhang, D.; Chang, J. *Mater. Chem. Phys.* **2009**, *118*, 379.
38. Liu, A.; Hong, Z.; Zhuang, X.; Chen, X.; Cui, Y.; Liu, Y.; Jing, X. *Acta Biomater.* **2008**, *4*, 1005.
39. Padmanabhann, K. S.; Gervaso, F.; Carrozzo, M.; Scalera, F.; Sannino, A.; Licciulli, A. *Ceram. Int.* **2013**, *39*, 619.
40. Teir, S.; Eloneva, S.; Zevenhoven, R. *Energy Convers. Manage.* **2005**, *46*, 2954.
41. Lau, K. T.; Gu, C.; Hui, D. *Compos. B Eng.* **2006**, *37*, 425.
42. Haplin, J. C. *J. Compos. Mater.* **1969**, *3*, 732.
43. Haplin, J. C.; Kardos, J. L. *Polym. Eng. Sci.* **1976**, *16*, 344.
44. Fornes, D. T.; Paul, R. D. *Polymer* **2003**, *44*, 4993.
45. Bernado, E.; Castellan, R.; Hreglich, S. *Ceram. Int.* **2007**, *33*, 27.